

Origin of the superconducting state in the collapsed tetragonal phase of KFe_2As_2

Daniel Guterding,* Steffen Backes, Harald O. Jeschke, and Roser Valentí
*Institut für Theoretische Physik, Goethe-Universität Frankfurt,
 Max-von-Laue-Straße 1, 60438 Frankfurt am Main, Germany*

Recently, KFe_2As_2 was shown to exhibit a structural phase transition from a tetragonal to a collapsed tetragonal phase under applied pressure of about 20 GPa. Surprisingly, the collapsed tetragonal phase hosts a superconducting state with $T_c \sim 12$ K, while the tetragonal phase is a $T_c \leq 3.4$ K superconductor. We argue that the key difference between the previously known non-superconducting collapsed tetragonal phase in BaFe_2As_2 , CaFe_2As_2 , EuFe_2As_2 , SrFe_2As_2 , and CaFe_2P_2 and the superconducting collapsed tetragonal phase in KFe_2As_2 is the qualitatively different electronic structure. While the collapsed phase in the former compounds features only electron pockets at the Brillouin zone boundary (M) and no hole pockets are present in the Brillouin zone center (Γ), the collapsed phase in KFe_2As_2 has both electron pockets at M and hole pockets at Γ . Our DFT+DMFT calculations show that effects of correlations on the electronic structure are minimal. Within a random phase approximation spin-fluctuation approach we calculate the superconducting pairing symmetry in the collapsed tetragonal phase of KFe_2As_2 and show that its electronic structure favors an s_{\pm} symmetry of the superconducting gap function. Finally, we argue that our results are also compatible with a change of sign of the Hall coefficient as observed experimentally.

PACS numbers: 71.15.Mb, 71.18.+y, 74.20.Pq, 74.70.Xa

I. INTRODUCTION

The family of AFe_2As_2 (A= Ba, Ca, Eu, K, Sr) superconductors, also called 122 materials, has been intensively investigated in the past due to their richness in structural, magnetic and superconducting phases upon doping or application of pressure^{1–6}. One phase whose properties have been recently scrutinized at length is the collapsed tetragonal (CT) phase present in BaFe_2As_2 , CaFe_2As_2 , EuFe_2As_2 , and SrFe_2As_2 under pressure and in CaFe_2P_2 ^{7–13}. The structural collapse of this phase has been shown to be assisted by the formation of As $4p_z$ -As $4p_z$ bonds between adjacent Fe-As layers giving rise to a bonding-antibonding splitting of the As p_z bands¹⁴. It has been argued that this phase does not support superconductivity due to the absence of hole cylinders at the Brillouin zone center and the corresponding suppression of spin fluctuations^{10,15,16}. However, recently Ying *et al.*¹⁷ investigated the hole-doped end member of $\text{Ba}_{1-x}\text{K}_x\text{Fe}_2\text{As}_2$, KFe_2As_2 , under high pressure and observed a boost of the superconducting critical pressure T_c up to 12 K precisely when the system undergoes a structural phase transition to a collapsed tetragonal phase at a pressure $P_c \sim 15$ GPa. These authors attributed this behavior to possible correlation effects. Moreover, measurements of the Hall coefficient showed a change from positive to negative sign upon pressure, indicating that the effective nature of charge carriers changes from holes to electrons with increasing pressure.

KFe_2As_2 has a few distinct features: at ambient pressure, the system shows superconductivity at $T_c = 3.4$ K and follows a V-shaped pressure dependence of T_c for moderate pressures with a local minimum at $P_c = 1.55$ GPa¹⁸. The origin of such behavior and the nature of the superconducting pairing symmetry is still un-

der debate^{19–25}. However, it has been established by a few experimental and theoretical investigations based on angle-resolved photoemission spectroscopy, de Haas van Alphen effect, and density functional theory combined with dynamical mean field theory (DFT+DMFT) calculations that correlation effects crucially influence the behavior of this system at $P = 0$ GPa^{26–33}. Application of pressure should nevertheless reduce the relative importance of correlations with respect to the bandwidth increase. In fact, recent DFT+DMFT studies on CaFe_2As_2 in the high-pressure collapsed tetragonal phase show that the topology of the Fermi surface is basically unaffected by correlations^{34,35}. One could argue though, that at ambient pressure CaFe_2As_2 is less correlated than KFe_2As_2 and therefore, in KFe_2As_2 correlation effects may be still significant at finite pressure.

In order to resolve these questions, we performed density functional theory (DFT) as well as DFT+DMFT calculations for KFe_2As_2 in the collapsed tetragonal phase. Our results show that the origin of superconductivity in the collapsed tetragonal phase in KFe_2As_2 lies in the qualitative changes in the electronic structure suffered under compression (Lifshitz transition) and correlations play only a minor role. Whereas in the tetragonal (TET) phase at $P = 0$ GPa KFe_2As_2 features predominantly only hole pockets at Γ , at $P \sim 15$ GPa in the collapsed tetragonal phase significant electron pockets emerge at the Brillouin zone boundary, which together with the hole pockets at Γ favor a superconducting state with s_{\pm} symmetry, as we show in our calculations of the superconducting gap function using the random phase approximation (RPA) spin-fluctuation approach. This scenario is distinct from the physics of the collapsed tetragonal phase in CaFe_2As_2 , where the hole pockets at Γ are absent. For comparison, we will present the susceptibility

of collapsed tetragonal CaFe_2As_2 . Our findings also suggest an explanation for the change of sign in the Hall coefficient upon entering the collapsed tetragonal phase in KFe_2As_2 .

II. METHODS

Density functional theory calculations were carried out using the all-electron full-potential local orbital (FPLO)³⁶ code. For the exchange-correlation functional we use the generalized gradient approximation (GGA) by Perdew, Burke, and Ernzerhof³⁷. All calculations were converged on $20 \times 20 \times 20$ k-point grids.

The structural parameters for the CT phase of KFe_2As_2 were taken from Ref. 17. We used the data points at $p \approx 21$ GPa, deep in the CT phase, where $a = 3.854$ Å and $c = 9.6$ Å. The fractional arsenic z-position ($z_{\text{As}} = 0.36795$) was determined *ab-initio* via structural relaxation using the FPLO code. For the CT phase of CaFe_2As_2 we used the experimental structural parameters from Ref. 38, which are the same as in our previous GGA+DMFT study³⁵. All Fe 3d orbitals are defined in a coordinate system rotated by 45° around the z-axis with respect to the conventional $I4/mmm$ unit cell.

For both CaFe_2As_2 and KFe_2As_2 we constructed 16-band tight-binding models using projective Wannier functions as implemented in FPLO³⁹. We keep the Fe 3d and As 4p states, which corresponds to an energy window of -6 eV to $+5$ eV in CaFe_2As_2 and -7 eV to $+6$ eV in KFe_2As_2 .

Subsequently, we unfold the 16-band model using our recently developed glide reflection unfolding technique⁴⁰, which produces an effective eight-band model of the three-dimensional one-Fe Brillouin zone.

We analyse these eight-band models using the 3D version of random phase approximation (RPA) spin-fluctuation theory⁴¹ with a Hamiltonian $H = H_0 + H_{\text{int}}$, where H_0 is the eight-band tight-binding Hamiltonian derived from the *ab-initio* calculations, while H_{int} is the Hubbard-Hund interaction, including the onsite intra (inter) orbital Coulomb interaction U (U'), the Hund's rule coupling J and the pair hopping energy J' . The arsenic states are kept in the entire calculation, but interactions are considered only between Fe 3d states. We assume spin rotation-invariant interaction parameters $U = 2.4$ eV, $U' = U/2$, and $J = J' = U/4$. These comparatively large values are necessary to bring the system close to the RPA instability, because of the large bandwidth in the collapsed tetragonal phase. Note however, that the symmetry of the superconducting gap in this system does not change, even if significantly reduced parameter values are considered.

The parameter values used in the RPA method are renormalized with respect to those in the DFT+DMFT method, because the electronic self-energy is neglected in the usual RPA scheme^{41,42}.

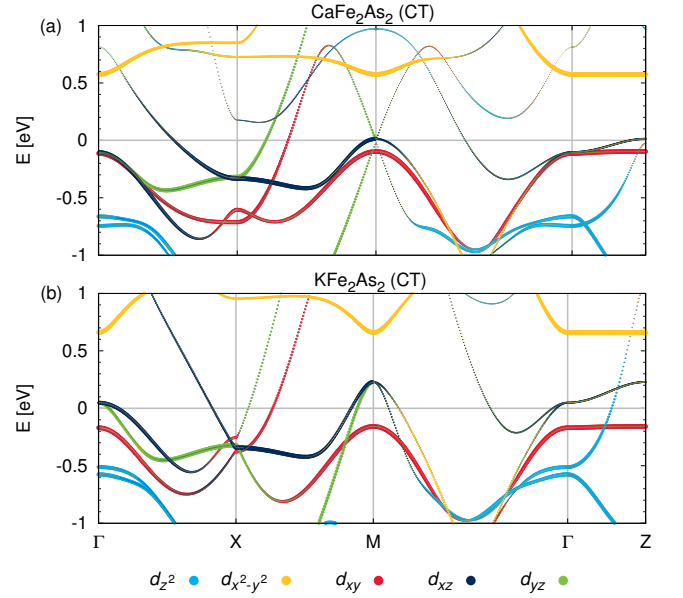


FIG. 1. (Color online) Electronic bandstructure of the collapsed tetragonal phase in (a) CaFe_2As_2 and (b) KFe_2As_2 . The path is chosen in the one-Fe equivalent Brillouin zone. The colors indicate the weights of Fe 3d states.

The non-interacting static susceptibility in orbital-space is defined by Eq. (1), where matrix elements $a_\mu^s(\vec{k})$ resulting from the diagonalization of the initial Hamiltonian H_0 connect orbital and band-space denoted by indices s and μ respectively. The E_μ are the eigenvalues of H_0 and $f(E)$ is the Fermi function.

$$\chi_{st}^{pq}(\vec{q}) = -\frac{1}{N} \sum_{\vec{k}, \mu, \nu} a_\mu^s(\vec{k}) a_\mu^{p*}(\vec{k}) a_\nu^q(\vec{k} + \vec{q}) a_\nu^{t*}(\vec{k} + \vec{q}) \times \frac{f(E_\nu(\vec{k} + \vec{q})) - f(E_\mu(\vec{k}))}{E_\nu(\vec{k} + \vec{q}) - E_\mu(\vec{k})} \quad (1)$$

The observable static susceptibility is defined as the sum over all elements χ_{aa}^{bb} of the full tensor (eq. 2).

$$\chi(\vec{q}) = \frac{1}{2} \sum_{a,b} \chi_{aa}^{bb}(\vec{q}) \quad (2)$$

The calculated static susceptibility tensor χ_{st}^{pq} measures strength and wave-vector dependence of spin-fluctuations in the investigated compound. The effective interaction in the singlet pairing channel is then constructed from the static susceptibility χ_{st}^{pq} via the multi-orbital RPA procedure. Both the original and effective interaction are discussed, e.g. in Ref. 43.

For the calculation of the susceptibility we used $30 \times 30 \times 10$ k-point grids and an inverse temperature of $\beta = 40$ eV⁻¹. The pairing interaction is constructed using ~ 800 points on the three-dimensional Fermi surface. We have shown previously that our implementation is capable of capturing effects of fine variations of shape and orbital character of the Fermi surface⁴⁴.

In order to estimate the strength of local electronic correlations in collapsed tetragonal KFe_2As_2 , we performed fully charge self-consistent DFT+DMFT calculations. We used the same method as described in Ref. 33. The DFT calculation was performed by the WIEN2K⁴⁵ implementation of the full-potential linear augmented plane wave (FLAPW) method in the local density approximation (LDA) with 726 k -points in the irreducible Brillouin zone. The Bloch wave functions are projected to the localized Fe 3d orbitals as described in Refs. 46 and 47. The energy window for projection was chosen from -7 to $+13$ eV, with the lower boundary lying in a gap in the density of states. For the solution of the DMFT impurity problem the continuous-time quantum Monte Carlo method in the hybridization expansion⁴⁸ as implemented in the ALPS^{49,50} project was employed. We used a temperature of 290 K, i.e. an inverse temperature $\beta = 40$ eV⁻¹. The interaction parameters are defined in terms of Slater integrals⁵¹ with an on-site Coulomb interaction $U = 4$ eV and Hund's rule coupling $J = 0.8$ eV. As the double counting correction we used the fully localized limit^{52,53} (FLL) scheme. Before the continuation of the imaginary-frequency selfenergy to the real axis by stochastic analytic continuation⁵⁴, the calculation was converged with 20×10^6 Monte-Carlo sweeps for the solution of the impurity model. The mass-renormalizations are directly calculated from the analytically continued real part of the impurity self-energy $\Sigma(\omega)$ via

$$\frac{m^*}{m_{\text{LDA}}} = 1 - \left. \frac{\partial \text{Re } \Sigma(\omega)}{\partial \omega} \right|_{\omega \rightarrow 0}. \quad (3)$$

III. RESULTS

We first calculated the electronic bandstructure in the collapsed tetragonal phase of CaFe_2As_2 and KFe_2As_2 (Fig. 1). The bandstructure results already reveal a striking difference between the CT phases of CaFe_2As_2 and KFe_2As_2 : while the former does not feature hole bands crossing the Fermi level at Γ and only one band barely crossing the Fermi level at M ($\pi, \pi, 0$), the latter does feature hole-pockets at both Γ and M in the one-Fe equivalent Brillouin zone. The reason for this difference in electronic structure is that KFe_2As_2 is strongly hole-doped compared to CaFe_2As_2 .

In Fig. 2 we show the Fermi surface in the one-Fe equivalent Brillouin zone. In both cases, the Fermi surface is dominated by Fe $3d_{xz/yz}$ character. The hole cylinders in KFe_2As_2 span the entire k_z direction of the Brillouin zone, while only a small three-dimensional hole-pocket is present in CaFe_2As_2 . For KFe_2As_2 the hole-pockets at M ($\pi, \pi, 0$) and the electron pockets at X ($\pi, 0, 0$) are clearly nested, while no nesting is observed for CaFe_2As_2 . It is important to note here, that the folding vector in the 122 family of iron-based superconductors is (π, π, π) , so that the hole-pockets at M ($\pi, \pi, 0$)

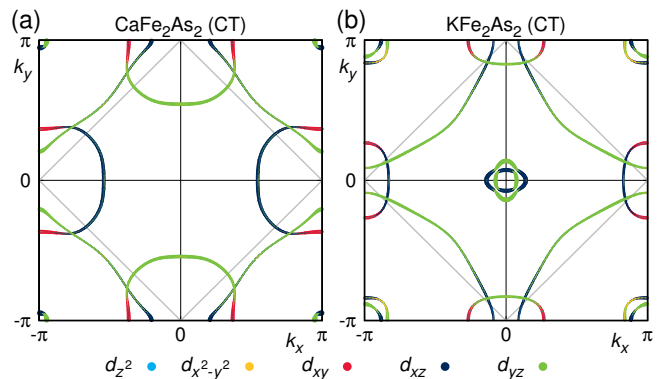


FIG. 2. (Color online) Fermi surface of the collapsed tetragonal phase in (a) CaFe_2As_2 and (b) KFe_2As_2 at $k_z = 0$. The full plot spans the one-Fe equivalent Brillouin zone, while the area enclosed by the grey lines is the two-Fe equivalent Brillouin zone. The colors indicate the weights of Fe 3d states.

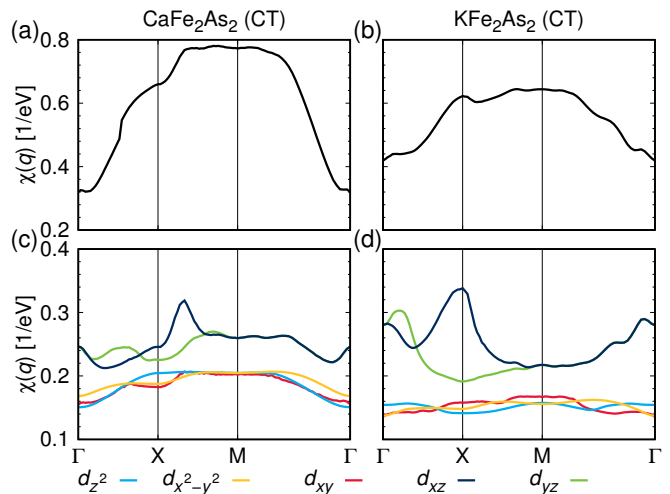


FIG. 3. (Color online) Summed static susceptibility (top) and its diagonal components χ_{aa}^{aa} (bottom) in the eight-band tight-binding model for [(a) and (c)] CaFe_2As_2 and [(b) and (d)] KFe_2As_2 in the one-Fe Brillouin zone. The colors identify the Fe 3d states.

will be located at Z ($0, 0, \pi$) after unfolding the bands to the effective one-Fe picture⁴⁰.

After qualitatively identifying the difference between the CT phases of CaFe_2As_2 and KFe_2As_2 , we calculate the non-interacting static susceptibility to verify that the better nesting of KFe_2As_2 generates stronger spin-fluctuations (Fig. 3). At first glance, the observable static susceptibility is larger in CaFe_2As_2 than in KFe_2As_2 , which would naively correspond to a stronger pairing interaction. A key difference is however revealed upon investigation of the largest elements, i.e. the diagonal entries χ_{aa}^{aa} . These show that in CaFe_2As_2 the susceptibility has broad plateaus, while in KFe_2As_2 the susceptibility has a strong peak at X ($\pi, 0, 0$) in the one-Fe Brillouin zone, which corresponds to the usual s_{\pm} pairing scenario that relies on electron-hole nesting. In CaFe_2As_2

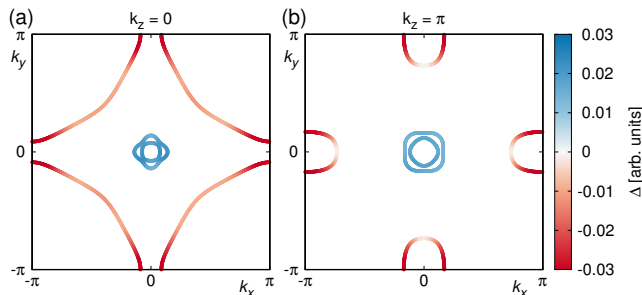


FIG. 4. (Color online) Leading superconducting gap function of the eight-band model in the one-Fe Brillouin zone of KFe_2As_2 in the CT phase at (a) $k_z = 0$ and (b) $k_z = \pi$.

TABLE I. Mass renormalizations m^*/m_{LDA} of the Fe $3d$ orbitals in the collapsed tetragonal phase of KFe_2As_2 calculated with the LDA+DMFT method.

d_{z^2}	$d_{x^2-y^2}$	d_{xy}	$d_{xz/yz}$
1.318	1.309	1.319	1.445

the pairing interaction is highly frustrated because there is no clear peak in favor of one pairing channel.

The leading superconducting gap function of KFe_2As_2 in the CT phase is shown in Fig. 4. As expected from our susceptibility calculations, the pairing symmetry is s -wave with a sign-change between electron and hole-pockets. While the superconducting gap is nodeless in the $k_z = 0$ plane, the $k_z = \pi$ plane does show nodes where the orbital character changes from Fe $3d_{xz/yz}$ to Fe $3d_{xy}$. Note that this $k_z = \pi$ structure of the superconducting gap is exactly the same as in the well studied LaFeAsO compound⁴¹, which shows that the CT phase of KFe_2As_2 closely resembles usual iron-based superconductors although it is much more three-dimensional than, e.g. in LaFeAsO . If tetragonal KFe_2As_2 is a d -wave superconductor as some authors propose^{20,21}, our results suggest that the Lifshitz transition, which occurs upon entering the collapsed tetragonal phase, changes the symmetry of the superconducting gap function from d -wave (TET) to s -wave (CT). The possible simultaneous change of pairing symmetry, density of states and T_c potentially opens up new routes to understanding their quantitative connection.

Furthermore, we estimated the strength of local correlations in collapsed tetragonal KFe_2As_2 . These are characterized by the mass-renormalizations m^*/m_{LDA} calculated from the LDA+DMFT method (Table I). The obtained values show that local electronic correlations in the collapsed tetragonal phase of KFe_2As_2 are comparable to those of CaFe_2As_2 in the collapsed tetragonal phase^{34,35}. As in CaFe_2As_2 , the effects of local electronic correlations on the Fermi surface are small.

The only deviation from the DFT Fermi surface is the closing of the hole cylinders shortly before Γ . As this change only affects a small fraction of the Brillouin zone around $k_z = 0$, and the relevant electron-hole nesting takes place at $k_z = \pi$, our superconducting pairing calculations based on the DFT bandstructure should be robust with respect to the effects of correlations. The higher T_c of the collapsed phase in absence of strong correlations raises the question how important strong correlations are in general for iron-based superconductivity. This issue demands further investigation.

Finally, the change of dominant charge carriers from hole to electron-like states measured in the Hall-coefficient under pressure¹⁷ is naturally explained from our calculated Fermi surfaces. While KFe_2As_2 is known to show only hole-pockets at zero pressure, the collapsed tetragonal phase features also large electron pockets. On a small fraction of these electron pockets, the dominating orbital character is Fe $3d_{xy}$ (Fig. 2). It was shown in Ref. 55 that quasiparticle lifetimes on the Fermi surface can be very anisotropic and long-lived states are favored where marginal orbital characters appear. As Fe $3d_{xy}$ character is only present on the electron pockets, they can be expected to have a significant contribution to transport.

IV. SUMMARY

We have shown that the electronic structure of the collapsed tetragonal phase of KFe_2As_2 qualitatively differs from that of other known collapsed materials. Upon entering the collapsed tetragonal phase, the Fermi surface of KFe_2As_2 undergoes a Lifshitz transition with electron pockets appearing at the Brillouin zone boundary, which are nested with the hole pockets at the Brillouin zone center. Thus, the spin-fluctuations in collapsed tetragonal KFe_2As_2 resemble those of other iron-based superconductors in non-collapsed phases and the superconducting gap function assumes the well-known s_{\pm} symmetry. This is in contrast to other known materials in the collapsed tetragonal phase, like CaFe_2As_2 , where hole pockets at the Brillouin zone center are absent and no superconductivity is favored. Based on our LDA+DMFT calculations, the collapsed tetragonal phase of KFe_2As_2 is significantly less correlated than the tetragonal phase, and mass enhancements are comparable to the CT phase of CaFe_2As_2 . Finally, we suggest that the change of dominant charge carriers from hole to electron-like can be explained from anisotropic quasiparticle lifetimes.

ACKNOWLEDGMENTS

We thank the Deutsche Forschungsgemeinschaft for financial support through Grant No. SPP 1458.

- * guterding@itp.uni-frankfurt.de
- ¹ M. Rotter, M. Tegel, and D. Johrendt, *Superconductivity at 38 K in the Iron Arsenide $(\text{Ba}_{1-x}\text{K}_x)\text{Fe}_2\text{As}_2$* , Phys. Rev. Lett. **101**, 107006 (2008).
 - ² S. A. J. Kimber, A. Kreyssig, Y. Z. Zhang, H. O. Jeschke, R. Valenti, F. Yokaichiya, E. Colombier, J. Yan, T. C. Hansen, T. Chatterji, R. J. McQueeney, P. C. Canfield, A. I. Goldman, and D. N. Argyriou, *Similarities between structural distortions under pressure and chemical doping in superconducting BaFe_2As_2* , Nat. Mater. **8**, 471 (2009).
 - ³ J. Paglione and R. L. Greene, *High-temperature superconductivity in iron-based materials*, Nat. Phys. **6**, 645 (2010).
 - ⁴ E. Gati, S. Köhler, D. Guterding, B. Wolf, S. Knöner, S. Ran, S. L. Bud'ko, P. C. Canfield, and M. Lang, *Hydrostatic-pressure tuning of magnetic, nonmagnetic, and superconducting states in annealed $\text{Ca}(\text{Fe}_{1-x}\text{Co}_x)_2\text{As}_2$* , Phys. Rev. B **86**, 220511(R) (2012).
 - ⁵ S. Lee, J. Jiang, Y. Zhang, C.W. Bark, J. D. Weiss, C. Tarantini, C. T. Nelson, H.W. Jang, C. M. Folkman, S. H. Baek, A. Polyanskii, D. Abrahimov, A. Yamamoto, J.W. Park, X. Q. Pan, E. E. Hellstrom, D. C. Larbalestier and C. B. Eom, *Template engineering of Co-doped BaFe_2As_2 single-crystal thin films*, Nat. Mater. **9**, 397 (2010).
 - ⁶ A. Leithe-Jasper, W. Schnelle, C. Geibel, and H. Rosner, *Superconducting State in $\text{SrFe}_{2-x}\text{Co}_x\text{As}_2$ by Internal Doping of the Iron Arsenide Layers*, Phys. Rev. Lett. **101**, 207004 (2008).
 - ⁷ W. Uchaya, A. Stemshorn, G. Tsoi, Y. K. Vohra, A. S. Sefat, B. C. Sales, K. M. Hope, and S. T. Weir, *Collapsed tetragonal phase and superconductivity of BaFe_2As_2 under high pressure*, Phys. Rev. B **82**, 144118 (2010).
 - ⁸ N. Ni, S. Nandi, A. Kreyssig, A. I. Goldman, E. D. Mun, S. L. Bud'ko, and P. C. Canfield, *First-order structural phase transition in CaFe_2As_2* , Phys. Rev. B **78**, 014523 (2008).
 - ⁹ Y.-Z. Zhang, H. C. Kandpal, I. Opahle, H. O. Jeschke, and R. Valenti, *Microscopic origin of pressure-induced phase transitions in the iron pnictide superconductors AFe_2As_2 : An ab initio molecular dynamics study*, Phys. Rev. B **80**, 094530 (2009).
 - ¹⁰ R. S. Dhaka, R. Jiang, S. Ran, S. L. Bud'ko, P. C. Canfield, B. N. Harmon, A. Kaminski, M. Tomic, R. Valenti, and Y. Lee *Dramatic changes in the electronic structure upon transition to the collapsed tetragonal phase in CaFe_2As_2* Phys. Rev. B **89**, 020511(R) (2014).
 - ¹¹ D. Kasinathan, M. Schmitt, K. Koepernik, A. Ormeci, K. Meier, U. Schwarz, M. Hanfland, C. Geibel, Y. Grin, A. Leithe-Jasper, and H. Rosner, *Symmetry-preserving lattice collapse in tetragonal $\text{SrFe}_{2-x}\text{Ru}_x\text{As}_2$ ($x=0,0.2$): A combined experimental and theoretical study*, Phys. Rev. B **84**, 054509 (2011).
 - ¹² W. Uchaya, G. Tsoi, Y. K. Vohra, M. A. McGuire, A. S. Sefat, B. C. Sales, D. Mandrus, and S. T. Weir, *Anomalous compressibility effects and superconductivity of EuFe_2As_2 under high pressures*, J. Phys.: Condens. Matter **22**, 292202 (2010).
 - ¹³ A. I. Coldea, C. M. J. Andrew, J. G. Analytis, R. D. McDonald, A. F. Bangura, J.-H. Chu, I. R. Fisher, and A. Carrington, *Topological Change of the Fermi Surface in Ternary Iron Pnictides with Reduced c/a Ratio: A de Haas-van Alphen Study of CaFe_2P_2* , Phys. Rev. Lett. **103**, 026404 (2009).
 - ¹⁴ T. Yildirim, *Strong Coupling of the Fe-Spin State and the As-As Hybridization in Iron-Pnictide Superconductors from First-Principle Calculations*, Phys. Rev. Lett. **102**, 037003 (2009).
 - ¹⁵ D. K. Pratt, Y. Zhao, S. A. J. Kimber, A. Hiess, D. N. Argyriou, C. Broholm, A. Kreyssig, S. Nandi, S. L. Bud'ko, N. Ni, P. C. Canfield, R. J. McQueeney, and A. I. Goldman, *Suppression of antiferromagnetic spin fluctuations in the collapsed phase of CaFe_2As_2* , Phys. Rev. B **79**, 060510(R) (2009).
 - ¹⁶ J. H. Soh, G. S. Tucker, D. K. Pratt, D. L. Abernathy, M. B. Stone, S. Ran, S. L. Bud'ko, P. C. Canfield, A. Kreyssig, R. J. McQueeney, and A. I. Goldman, *Inelastic Neutron Scattering Study of a Nonmagnetic Collapsed Tetragonal Phase in Nonsuperconducting CaFe_2As_2 : Evidence of the Impact of Spin Fluctuations on Superconductivity in the Iron-Arsenide Compounds*, Phys. Rev. Lett. **111**, 227002 (2013).
 - ¹⁷ J.-J. Ying, L.-Y. Tang, V. V. Struzhkin, H.-K. Mao, A. G. Gavriluk, A.-F. Wang, X.-H. Chen, and X.-J. Chen, *Tripling the critical temperature of KFe_2As_2 by carrier switch*, arXiv:1501.00330 (unpublished).
 - ¹⁸ F. F. Tafti, A. Juneau-Fecteau, M.-È. Delage, S. René de Cotret, J-Ph. Reid, A. F. Wang, X-G. Luo, X. H. Chen, N. Doiron-Leyraud, and L. Taillefer, *Sudden reversal in the pressure dependence of T_c in the iron-based superconductor KFe_2As_2* , Nat. Phys. **9**, 349 (2013).
 - ¹⁹ K. Okazaki, Y. Ota, Y. Kotani, W. Malaeb, Y. Ishida, T. Shimojima, T. Kiss, S. Watanabe, C-T. Chen, K. Kihou, C-H. Lee, A. Iyo, H. Eisaki, T. Saito, H. Fukazawa, Y. Kohori, K. Hashimoto, T. Shibauchi, Y. Matsuda, H. Ikeda, H. Miyahara, R. Arita, A. Chainani, and S. Shin, *Octet-Line Node Structure of Superconducting Order Parameter in KFe_2As_2* , Science **337**, 1314 (2012).
 - ²⁰ R. Thomale, Ch. Platt, W. Hanke, J. Hu, B. A. Bernevig, *Exotic d-Wave Superconducting State of Strongly Hole-Doped $\text{K}_x\text{Ba}_{1-x}\text{Fe}_2\text{As}_2$* , Phys. Rev. Lett. **107**, 117001 (2011).
 - ²¹ J-Ph. Reid, M. A. Tanatar, A. Juneau-Fecteau, R. T. Gordon, S. René de Cotret, N. Doiron-Leyraud, T. Saito, H. Fukazawa, Y. Kohori, K. Kihou, C-H. Lee, A. Iyo, H. Eisaki, R. Prozorov, and L. Taillefer, *Universal Heat Conduction in the Iron Arsenide Superconductor KFe_2As_2 : Evidence of a d-Wave State*, Phys. Rev. Lett. **109**, 087001 (2012).
 - ²² S. Maiti, M. M. Korshunov, T. A. Maier, P. J. Hirschfeld, A. V. Chubukov, *Evolution of the Superconducting State of Fe-Based Compounds with Doping*, Phys. Rev. Lett. **107**, 147002 (2012).
 - ²³ K. Suzuki, H. Usui, and K. Kuroki, *Spin fluctuations and unconventional pairing in KFe_2As_2* , Phys. Rev. B **84**, 144514 (2011).
 - ²⁴ F. F. Tafti, J. P. Clancy, M. Lapointe-Major, C. Collignon, S. Faucher, J. A. Sears, A. Juneau-Fecteau, N. Doiron-Leyraud, A. F. Wang, X.-G. Luo, X. H. Chen, S. Desgreniers, Y-J. Kim, and L. Taillefer, *Sudden reversal in the pressure dependence of T_c in the iron-based superconductor CsFe_2As_2 : A possible link between inelastic scattering and pairing symmetry*, Phys. Rev. B **89**, 134502 (2014).
 - ²⁵ F. F. Tafti, A. Ouellet, A. Juneau-Fecteau, S. Faucher, M. Lapointe-Major, N. Doiron-Leyraud, A. F. Wang,

- X. G. Luo, X. H. Chen, and L. Taillefer, *Universal V-shaped temperature-pressure phase diagram in the iron-based superconductors KFe_2As_2 , $RbFe_2As_2$, and $CsFe_2As_2$* , arXiv:1412.6196 (unpublished).
- ²⁶ T. Terashima, M. Kimata, N. Kurita, H. Satsukawa, A. Harada, K. Hazama, M. Imai, A. Sato, K. Kihou, C-H. Lee, H. Kito, H. Eisaki, A. Iyo, T. Saito, H. Fukazawa, Y. Kohori, H. Harima, and S. Uji, *Fermi Surface and Mass Enhancements in KFe_2As_2 from de Haas-van Alphen Effect Measurements*, J. Phys. Soc. Jpn. **79**, 053702 (2010).
 - ²⁷ T. Yoshida, I. Nishi, A. Fujimori, M. Yi, R. G. Moore, D-H. Lu, Z-X. Shen, K. Kihou, P. M. Shirage, H. Kito, C-H. Lee, A. Iyo, H. Eisaki, and H. Harima, *Fermi surfaces and quasi-particle band dispersions of the iron pnictide superconductor KFe_2As_2 observed by angle-resolved photoemission spectroscopy*, J. Phys. Chem. Solids **72**, 465 (2011).
 - ²⁸ M. Kimata, T. Terashima, N. Kurita, H. Satsukawa, A. Harada, K. Kodama, K. Takehana, Y. Imanaka, T. Takamasu, K. Kihou, C-H. Lee, H. Kito, H. Eisaki, A. Iyo, H. Fukazawa, Y. Kohori, H. Harima, and S. Uji, *Cyclotron Resonance and Mass Enhancement by Electron Correlation in KFe_2As_2* , Phys. Rev. Lett. **107**, 166402 (2011).
 - ²⁹ T. Sato, N. Nakayama, Y. Sekiba, P. Richard, Y-M. Xu, S. Souma, T. Takahashi, G. F. Chen, J. L. Luo, N. L. Wang, and H. Ding, *Band Structure and Fermi Surface of an Extremely Overdoped Iron-Based Superconductor KFe_2As_2* , Phys. Rev. Lett. **103**, 047002 (2009).
 - ³⁰ T. Yoshida, S. Ideta, I. Nishi, A. Fujimori, M. Yi, R. G. Moore, S. K. Mo, D-H. Lu, Z-X. Shen, Z. Hussain, K. Kihou, P. M. Shirage, H. Kito, C-H. Lee, A. Iyo, H. Eisaki, and H. Harima, *Orbital character and electron correlation effects on two- and three-dimensional Fermi surfaces in KFe_2As_2 revealed by angle-resolved photoemission spectroscopy*, Front. Physics **2**, 17 (2014).
 - ³¹ T. Terashima, N. Kurita, M. Kimata, M. Tomita, S. Tsuchiya, M. Imai, A. Sato, K. Kihou, C-H. Lee, H. Kito, H. Eisaki, A. Iyo, T. Saito, H. Fukazawa, Y. Kohori, H. Harima, and S. Uji, *Fermi surface in KFe_2As_2 determined via de Haas-van Alphen oscillation measurements*, Phys. Rev. B **87**, 224512 (2013).
 - ³² Z. P. Yin, K. Haule, and G. Kotliar, *Kinetic frustration and the nature of the magnetic and paramagnetic states in iron pnictides and iron chalcogenides*, Nat. Mater. **10**, 932 (2011).
 - ³³ S. Backes, D. Guterding, H. O. Jeschke, and R. Valentí, *Electronic structure and de Haas-van Alphen frequencies in KFe_2As_2 within LDA+DMFT*, New J. Phys. **16**, 085025 (2014).
 - ³⁴ S. Mandal, R. E. Cohen, and K. Haule, *Pressure suppression of electron correlation in the collapsed tetragonal phase of $CaFe_2As_2$: A DFT-DMFT investigation*, Phys. Rev. B **90**, 060501(R) (2014).
 - ³⁵ J. Diehl, S. Backes, D. Guterding, H. O. Jeschke, and R. Valentí, *Correlation effects in the tetragonal and collapsed tetragonal phase of $CaFe_2As_2$* , Phys. Rev. B **90**, 085110 (2014).
 - ³⁶ K. Koepnick and H. Eschrig, *Full-potential nonorthogonal local-orbital minimum-basis band-structure scheme*, Phys. Rev. B **59**, 1743 (1999); <http://www.FPLO.de>
 - ³⁷ J. P. Perdew, K. Burke, and M. Ernzerhof, *Generalized Gradient Approximation Made Simple*, Phys. Rev. Lett. **77**, 3865 (1996).
 - ³⁸ A. Kreyssig, M. A. Green, Y. Lee, G. D. Samolyuk, P. Zajdel, J. W. Lynn, S. L. Bud'ko, M. S. Torikachvili, N. Ni, S. Nandi et al., *Pressure-induced volume-collapsed tetragonal phase of $CaFe_2As_2$ as seen via neutron scattering*, Phys. Rev. B **78**, 184517 (2008).
 - ³⁹ H. Eschrig and K. Koepnick, *Tight-binding models for the iron-based superconductors*, Phys. Rev. B **80**, 104503 (2009).
 - ⁴⁰ M. Tomić, H. O. Jeschke, and R. Valentí, *Unfolding of electronic structure through induced representations of space groups: Application to Fe-based superconductors*, Phys. Rev. B **90**, 195121 (2014).
 - ⁴¹ S. Graser, T. A. Maier, P. J. Hirschfeld, and D. J. Scalapino, *Near-degeneracy of several pairing channels in multiorbital models for the Fe pnictides*, New J. Phys. **11**, 025016 (2009).
 - ⁴² K. Kuroki, H. Usui, S. Onari, R. Arita, and H. Aoki, *Pnictogen height as a possible switch between high- T_c nodeless and low- T_c nodal pairings in the iron-based superconductors*, Phys. Rev. B **79**, 224511 (2009).
 - ⁴³ P. J. Hirschfeld, M. M. Korshunov, and I. I. Mazin, *Gap symmetry and structure of Fe-based superconductors*, Rep. Prog. Phys. **74**, 124508 (2011).
 - ⁴⁴ D. Guterding, H. O. Jeschke, P. J. Hirschfeld, and R. Valentí, *Unified picture of the doping dependence of superconducting transition temperatures in alkali metal/ammonia intercalated FeSe*, Phys. Rev. B (in press) (2015).
 - ⁴⁵ P. Blaha, K. Schwarz, G. K. H. Madsen, D. Kvasnicka, and J. Luitz, *An Augmented Plane Wave Plus Local Orbitals Program for Calculating Crystal Properties* (Karlheinz Schwarz, Techn. Universität Wien, Austria) (2001).
 - ⁴⁶ M. Aichhorn, L. Pourovskii, V. Vildosola, M. Ferrero, O. Parcollet, T. Miyake, A. Georges, and S. Biermann, *Dynamical mean-field theory within an augmented plane-wave framework: Assessing electronic correlations in the iron pnictide $LaFeAsO$* , Phys. Rev. B **80**, 085101 (2009).
 - ⁴⁷ J. Ferber, K. Foyevtsova, H. O. Jeschke, and R. Valentí, *Unveiling the microscopic nature of correlated organic conductors: The case of κ -(ET)₂Cu[N(CN)₂Br_xCl_{1-x}]*, Phys. Rev. B **89**, 205106 (2014).
 - ⁴⁸ P. Werner, A. Comanac, L. de' Medici, M. Troyer, and A. J. Millis, *Continuous-Time Solver for Quantum Impurity Models*, Phys. Rev. Lett. **97**, 076405 (2006).
 - ⁴⁹ B. Bauer, L. D. Carr, H. G. Evertz, A. Feiguin, J. Freire, S. Fuchs, L. Gamper, J. Gukelberger, E. Gull, S. Guertler et al., *The ALPS project release 2.0: open source software for strongly correlated systems*, J. Stat. Mech. Theory Exp., P05001 (2011).
 - ⁵⁰ E. Gull, P. Werner, S. Fuchs, B. Surer, T. Pruschke, and M. Troyer, *Continuous-time quantum Monte Carlo impurity solvers*, Comput. Phys. Commun. **182**, 1078 (2011).
 - ⁵¹ A. I. Liechtenstein, V. I. Anisimov, and J. Zaanen, *Density-functional theory and strong interactions: Orbital ordering in Mott-Hubbard insulators*, Phys. Rev. B **52**, R5467(R) (1995).
 - ⁵² S. L. Dudarev, G. A. Botton, S. Y. Savrasov, C. J. Humphreys, and A. P. Sutton, *Electron-energy-loss spectra and the structural stability of nickel oxide: An LSDA+U study*, Phys. Rev. B **57**, 1505 (1998).
 - ⁵³ V. I. Anisimov, I. V. Solov'yev, M. A. Korotin, M. T. Czyzyk, and G. A. Sawatzky, *Density-functional theory and NiO photoemission spectra*, Phys. Rev. B **48**, 16929 (1993).
 - ⁵⁴ K. S. D. Beach, *Identifying the maximum entropy method as a special limit of stochastic analytic continuation*, arXiv:cond-mat/0403055 (unpublished) (2004).

- ⁵⁵ A. F. Kemper, M. M. Korshunov, T. P. Devereaux, J. N. Fry, H-P. Cheng, and P. J. Hirschfeld, *Anisotropic quasi-particle lifetimes in Fe-based superconductors*, Phys. Rev. B **83**, 184516 (2011).